Int J Clin Exp Pathol 2014;7(3):858-869
www.ijcep.com /ISSN:1936-2625/IJCEP1311068

Original Article

Coxsackievirus-induced acute neonatal central nervous system disease model

Lulu Wang[1*], Changyuan Dong[1], Dong-E Chen[2], Zhen Song[1*]

[1]Laboratory of Molecular Virus & Cancer, State Key Laboratory of Virology, Wuhan University School of Basic Medicine, Wuhan 430071, China; [2]Department of Epidemiology and Biostatistics, Wuhan University School of Public Health, Wuhan 430071, China. [*]Joint first authors.

Received November 27, 2013; Accepted January 3, 2014; Epub February 15, 2014; Published March 1, 2014

Abstract: Coxsackievirus B (CVB) is a significant pathogen that causes pediatric central nervous system disease with acute syndromes commonly. The onset of its infection was abrupt, and after recovery there usually will be severe mental sequelae. The disease model for research was not established by the way of natural infection, although there are various investigations about the CVB-induced central nervous system (CNS) diseases. Thus, we have established an acute neonatal CNS disease mice model by CVB orally infecting. This model imitated the natural infection route and focuses the onset of CNS disease, inducing severe infection and lesion in the hippocampus and cortex regions, and the stability of the model was demonstrated. A pathology score system was developed for quantitative pathology analysis, which standardizes the CNS pathology analysis by statistics analysis. By this model, the track of CVB penetrating the blood brain barrier in vivo has been captured. One of the experimental strains CVB3/Macocy, as a new variant, was isolated, and its genomic RNA was cloned. According to its nucleotide sequence, we have characterized its genomic structure and defined its genotype. Based on the sequence, some mutations which do not change the CVB-induced CNS damage have been found. The model is an effective tool for studies on CVB-induced CNS diseases.

Keywords: Coxsackievirus B, acute neonatal central nervous system disease, mouse model, strain Macocy

Introduction

Coxsackievirus B (CVB) belongs to the *Humen Enterovirus*, genus of the *Picornaviridae*. Historically, coxsackie viruses were sorted into A and B groups according to pathogenicity in newborn mice. Recent studies on the genomic RNA of enterovirus suggested that the viruses in one traditional group are genetically quite diverse, which has led to the adoption of a new taxonomy [1].

CVB causes the neonatal diseases in central nervous system (CNS) especially meningitis [2, 3] frequently because of the immaturity of their immune systems [4]. It is typically occurred with abrupt syndrome of fever, meningeal irritation, headache and photophobia at the stage of onset [5]. Traditionally, the CVB disease models were established through virus intraperitoneal injection [6, 7]. And for the establishment of CNS infection model, the intracranial injection was used [8]. But these ways of infection are not the real way for viral invasion. In fact, CVB infects naturally via fecal-oral transmission. It begins infection within the intestine, and proliferates in it. Thus the neonatal CNS disease model established via oral infection is more meaningful for the researches on CVB-induced CNS diseases comparing the other unnatural inoculation route.

The hippocampal pathology, especially dentate gyrus damage, and cortex regions pathology are related to schizophrenia and other neuropsychiatric illness [9-11]. Some of these illnesses are induced by enterovirus [12, 13]. In the CNS infection studies, the proposal of enterovirus can access the CNS through blood brain barrier (BBB) was based on the in vitro model of the epithelial barrier [14-16]. However, it is still unclear that how CVB accesses CNS in vivo.

This study focuses on the establishment of an acute CNS disease model by natural CVB infec-

Table 1. The sequence identities of CVB3/Macocy with the other 11 CVB3 strains

Strain	Accession Number[a]	Sequence Identity[b]	p Distance
28	AY752944	0.9972973	0.0027027
0	AY752945	0.9968919	0.0031081
P	AF231764	0.9967568	0.0032432
20	AY752946	0.9967563	0.0032437
31-1-93	AF231763	0.9954054	0.0045946
anonymous	M33854	0.9954054	0.0045946
Nancy	JN048468	0.9951450	0.0048550
PD	AF231765	0.9951351	0.0048649
Woodruff	U57056	0.9158108	0.0841892
GA	AY673831	0.8183905	0.1816095
MCH	EU144042	0.8013227	0.1986773

[a]These are accession numbers in Genbank. [b]The sequence identities were shown in decreasing order.

tion on neonatal mice at the onset phase, and demonstrated the reliability and stability of the model from the point of pathology and statistics analysis.

Materials and methods

Virus and cell culture

Two strains of CVB3 were used in this study. One virus strain, CVB3/Macocy, was isolated from an experiment mouse in our lab in 2007. The other strain CVB3/Nancy was from HuBei CDC in 2008. Vero cell monolayer were inoculated for proliferation and titration of virus, maintaining in Dulbecco's modified minimal essential medium (DMEM, Sigma) supplemented with 2 mmol/l L-glutamine and 10% calf serum at 37°C under 5.0% CO_2.

Isolation of Macocy strain

In the plaque assay, Vero cells were seeded in four 90-mm-diameter plates (1-2×10^5 cells/plate) and incubated at 37°C under 5.0% CO_2 for about 48 hours, at which time they reached about 90% confluence. Then, serial dilutions (10^5, 10^6, 10^7, 10^8 times) of Macocy strain suspension was inoculated onto Vero cell monolayer in a final volume of 1 ml per well. After about 1 hour of incubation, the supernatant was removed away, and the cell monolayer was overlaid with 15 ml of mixture (1.5% agarose, 10% calf serum, DMEM, neutral red). After about 1 day of incubation under normal culture conditions, the formations of cytopathic plaques were visualized in the 10^7 times dilution of virus stock. For virus isolation, a single plaque was gouged out, and the virus from the single plaque was proliferated on another Vero cell monolayer as previous description.

Virus quantification

$TCID_{50}$ assay was employed to quantify both strains which were cultured in two plates of 96 wells. When Vero cells formed monolayer, they were infected with virus suspension which was formerly sterilized by filtration. Both of the two strains virus suspensions were diluted producing 10-fold serial dilutions arranging from 10^{-1} to 10^{-10}. Each dilution was added to 8 wells with 100 μl/well. Meanwhile the left 16 wells (row11 and row12) of cells in each plate were cultured as the control group. At last, the two plates were placed at 37°C with 5% CO_2 and the cytopathic effect (CPE) was observed. While CPE appearing completely, the $TCID_{50}$ was calculated by Reed-Muench method.

Cloning of the virus RNA as cDNA fragments

The genomic RNA of the isolated virus was extracted by TRIzol reagent (Invitrogen). Further, full genomic cDNA was synthesized by First Strand cDNA Synthesis Kit (Fermentas). $Oligo(dT)_{18}$ Primer provided by the kit was used to synthesize the full genomic cDNA. On the basis of published Coxsackievirus B3/Nancy (GenBank accession number: M16572), 8 primer pairs were designed, synthesized and employed in cDNA amplifications (**Table 1**). Using genomic RNA as the template, 8 overlapping cDNA fragments were synthesized and amplified with RT-PCR. Then, the amplified cDNA fragments were isolated, digested by Sac II and Sac I, and ligated into Sac II-digested and Sac I-digested pBluescriptIISK (+) vector. By IPTG X-gal blue/white color selection test, the positive recombinant plasmids were chosen. At last, they were examined by PCR and restriction endonuclease detections subsequently.

Sequence analysis and molecular typing for Macocy strain

The inserted cDNA fragments were sequenced and they were read from both strands. Then, the sequence data were analyzed by BioEdit

7.0.8 software [17]. All of the 8 nucleotide sequences were spliced to a complete genomic nucleotide sequence. Furthermore, the 5'UTR, ORF, and 3'UTR were determined by sequence analysis. Moreover, to determine the species of Macocy in enterovirus, the complete nucleotide sequences of Macocy and the other 63 Human enterovirus strains were aligned by clustalW module in MEGA 5.04 [18]. The phylogenetic relationships and genetic distances were inferred by the Minimum Evolution method. The branch support of the phylogenetic tree was estimated by bootstrap analysis with 2000 pseudo-replicate data sets. Further, the genomic sequence identity between Macocy and other 11 CVB3 strains was calculated by Bioedit software pairwise alignment module. Besides, the processing sites of the ORF coded polyprotein of Macocy were determined by referring the other researches on the polyprotein processing of CVB3.

Mouse model

Neonatal BALB/c mice (randomized male and female) within 24 hours were acquired from Animal Center of Wuhan University and were bred and fed by aseptic milk under pathogen-free circumstances for 72 hours. The mock control group, the group Macocy (CVB3/Macocy strain) and group Nancy (CVB3/Nancy strain) were separated without air circulation among groups. The number of each group was 44. Virus inocula containing 5×10^5 $TCID_{50}$ of CVB3 Macocy and Nancy strains in 25 μl DMEM were administered to each group orally by micropipette with less than 1 μl of every feeding. The ingestion way of these mice was sucking. In this course, it is imperative to avoid the mice to spit out the inocula and ensure the volume dose. In 72 hours after inoculation, mice were observed at every 12 hours and the fatality was counted. 72 hours after, the living mice were dissected, and the brain tissues were harvested. Then, all the tissues were washed in phosphate buffer solution (PBS), and fixed in 10% formaldehyde.

Hematoxylin & eosin (H&E) and immunohistochemistry (IHC) assay

All the tissues were fixed in formalin, embedded in paraffin and sliced into sections at 3.5 μm. The sections were deparaffinized with two washes in xylene and sequential washed in alcohol. Then they were stained with hematoxylin solution, differentiated in 1% acid alcohol, immersed in 0.2% ammonia water and 0.5% eosin solution. At last, they were sequential dehydrated in alcohol and mounted with xylene. Each process was following with the wash in double distilled water (ddH_2O).

For detecting the CVB3 VP1 protein, the Monoclonal antibody Mab 948 (Millipore) was used as the primary antibody in IHC assay. 3.5 μm embedded tissue sections were incubated, deparaffinized in in xylene and sequential concentrated in alcohol. After antigen retrieval and blocking endogenous peroxidase, the sections were incubated with bovine serum albumin for blocking nonspecific staining. Subsequently, the primary monoclonal antibody, biotin-labeled goat anti-mouse antibody (1:200 final dilution; Vector Laboratories, Burlingame, CA) and avidin-biotin peroxidase complexes (1:25 final dilution; Vector Laboratories) were incubated one by one. Diaminobenzidine was applied as the final chromogen, and hematoxylin was the nuclear counterstain.

Pathology score

According to a pathology score system, each tissue's pathological lesion was scored. The pathology of every brain tissue was scored twice. The pathology of necrosis and inflammatory exudation were referenced. The degrees include mild, moderate and severe. The mild degree of pathology is manifested by tissue swelling and cells degeneration, which can be scored 1-2; the moderate degree is manifested by local necrosis which can be scored 3-4; the severe degree is manifested by submassive and massive necrosis which can be scored 5-6; no obvious pathology was scored 0; besides, every tissue could acquire 1-2 additional score in accordance with its inflammatory exudation, in which local exudation score 1 and massive exudation score 2. So, the score's range is 0-8. According to the significant pathological lesion criterion of score ≥3, we can count the pathological lesion rates.

Statistical analysis

The statistical analysis was employed by SPSS 17.0 for Windows, except for calculating group size and *power*. By the formula that are suitable for Chi-Square test with significance level $\alpha<0.05$ [19, 20] and by the formula that are suitable for Fisher's exact test with significance level $\alpha<0.05$ [21], the group size and *power* were calculated.

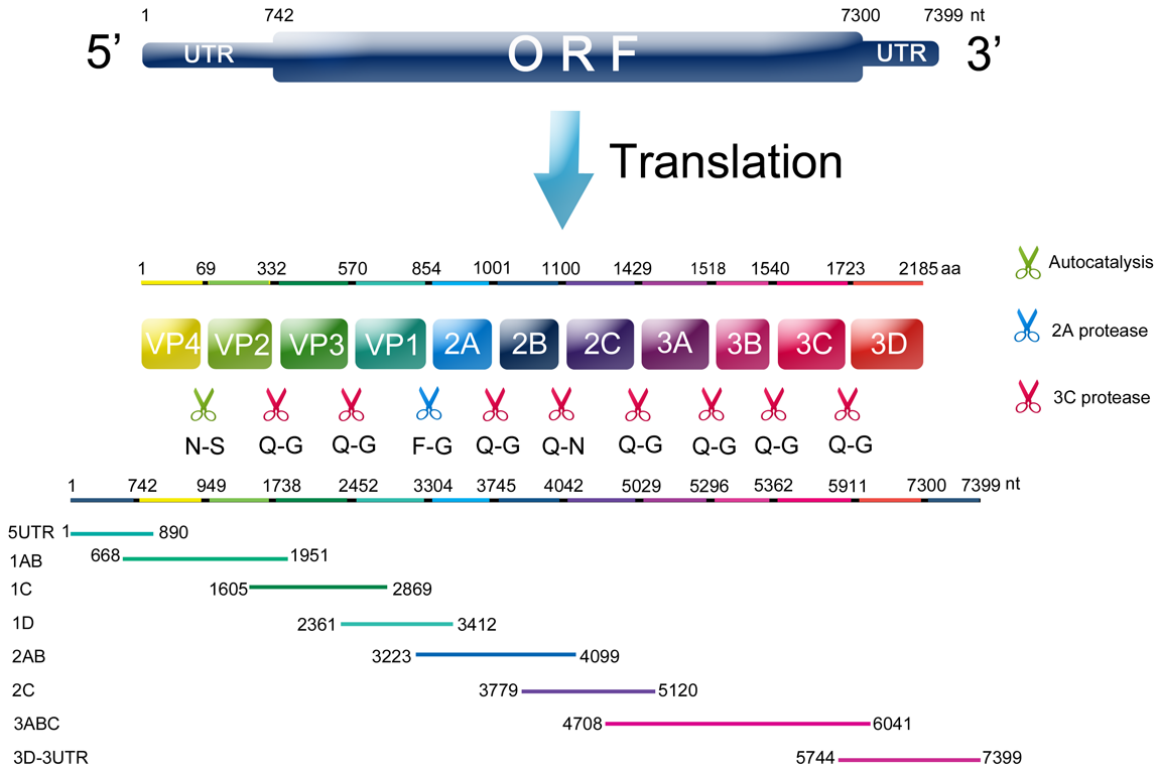

Figure 1. The genome scheme of CVB3/Macocy strain, the coded proteins, protein processing sites and PCR fragments. The numbers marked above the genome schema and two colored marked lines indicate the ranges of every division. The 11 mature proteins (from VP4 to 3D) were represented by different colors. Below the proteins, the 10 scissor icons marked the processing sites on the polyprotein, where green, blue and red scissors stand for autocatalysis of VP4 and VP2, 2A protease, and 3C protease respectively. At the bottom, the 8 PCR fragments were presented with their names at the left side, and the nucleotide range.

Chi-Square test for 2×2 contingency table has been used to assess the statistical significance of fatality rates and infection rates for group Macocy and group Nancy respectively with significant level $\alpha<0.05$.

Chi-Square test for 2×2 contingency-table method has been employed to assess the difference of fatality rate and pathological lesion rates for group Macocy versus Nancy with significance level $\alpha<0.05$. Fisher's exact test for 2×2 contingency-table method has been used to assess the difference of infection rates for group Macocy versus Nancy with significance level $\alpha<0.05$.

Result

Virus preparation and CVB3 nucleotide sequence description

The CVB3/Macocy strain was isolated by plaque assay from a single plaque. Tissue culture infectious dose 50 ($TCID_{50}$) of both of the CVB3/Macocy strain and CVB3/Nancy strain suspension were calculated respectively. Moreover, the genomic RNA of the new isolated CVB3 strain was extracted and full genomic cDNA was synthesized with the method of reverse transcription PCR (RT-PCR). 8 amplified cDNA fragments, which overlap and cover the whole genome of CVB3, were inserted in vectors. After sequencing and splicing, the complete nucleotide sequence of genomic cDNA was acquired (GenBank accession number: JQ040513). The length of the whole nucleotide is 7399nt and the open reading frame (ORF) is from 743nt to 7300nt encoding a polyprotein which owns 2185 residues. The 5'UTR and 3'UTR lay on the two terminals with a length of 742nt and 99nt respectively. The polyprotein processing site between VP4 and VP2 is N-S on the 69th amino acid. VP4 and VP2 are matured by autocatalysis. The site between VP1 and 2A is F-G on the 854th amino acid. VP1 and 2A are

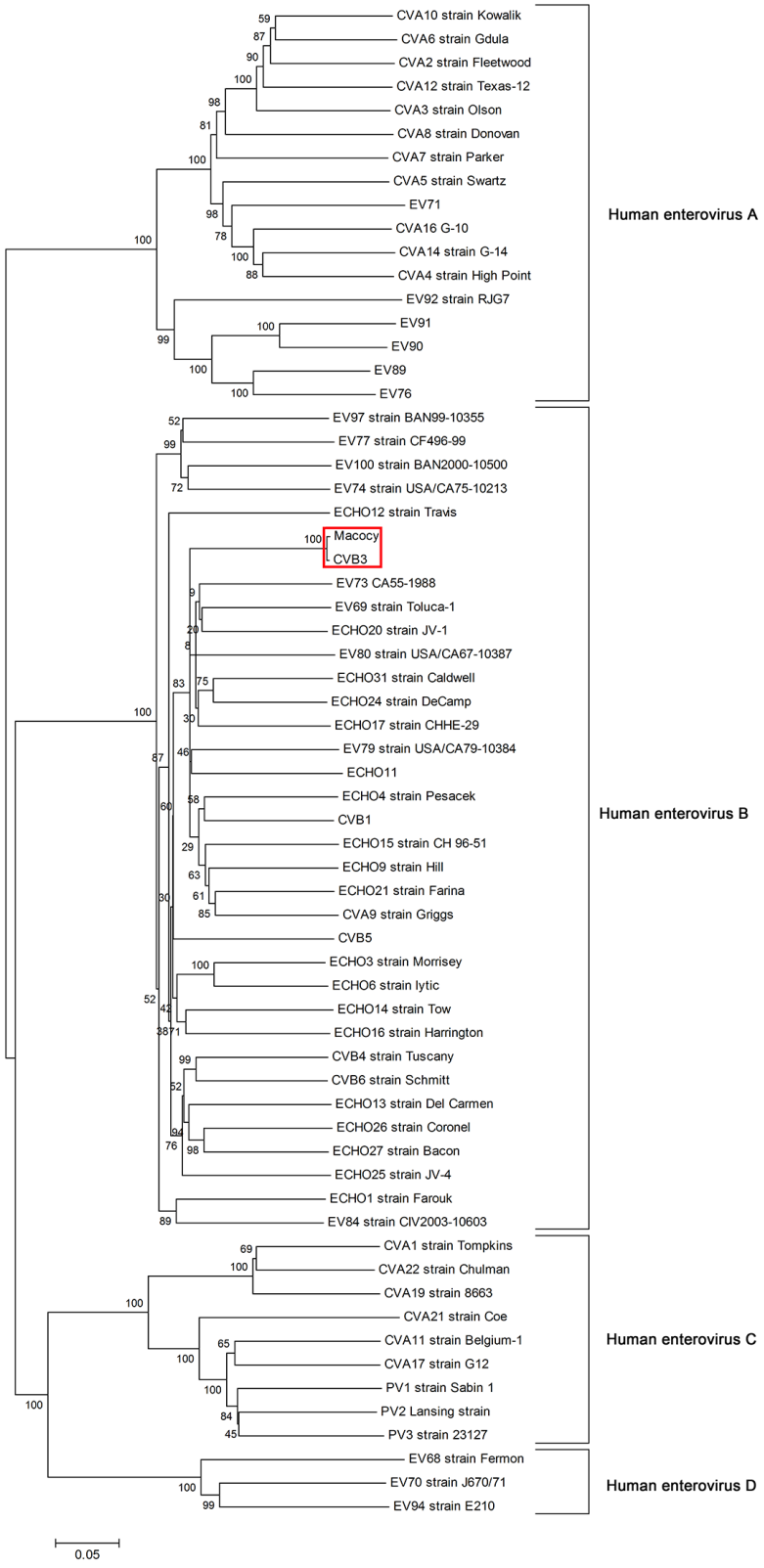

Figure 2. The phylogenetic relationship of the genome of strain Macocy and other Human enterovirus strains. The analysis was based on the complete genomic sequence. The numbers beside the branches are Minimum Evolution bootstrap values. The scale bar represents 0.05 substitutions per site. Strain Macocy and CVB3 were boxed off.

processed by 2A protease. The sites between VP2 and VP3, VP3 and VP1, 2A and 2B, 2C and 3A, 3A and 3B, 3B and 3C, 3C and 3D are Q-G on the 332nd, 570th, 1001st, 1429th, 1518th, 1540th, 1723rd amino acid respectively, and these proteins are processed by 3C protease respectively. The site between 2B and 2C is Q-N on the 1100th amino acid. 2B and 2C are processed by 3C protease too (**Figure 1**).

Molecular typing and sequence identity

The complete cDNA nucleotide sequence of strain Macocy and other 63 human enterovirus were compared by multi-alignment. Based on that, a phylogenetic tree was drawn. Evidently, in the phylogenetic tree, the 64 human enterovirus strains have been classified into four groups: human enterovirus A, human enterovirus B, human enterovirus C and human enterovirus D. The result is in accordance with the report of the International Committee on the Taxonomy of Viruses [1]. It is obvious that the strain Macocy shares the same position with CVB3 in Human enterovirus B, which has high bootstrap value support. It means that Macocy is a strain within CVB3 (**Figure 2**).

We also calculated the sequence identity between strain Macocy and other 11 CVB3 strains. Considering the CVB3 strains are closely related genomic sequences, the raw proportion comparison works fine when p value < 5% [22]. It shows that Macocy has the highest

Table 2. RT-PCR Primer Pairs

Primer Names[a]	Sites (nt)	Sequences (5'~3')[b]	Restriction Sites
5UTR-S	1~20	TATCCGCGGTTAAAACAGCCTGTGGGTTG	Sac II
5UTR-A	869~888	GCGGTCGACGGTCTTGAGTGAAATCCTGC	Sac I
1AB-S	666~690	GTCCCCGCGGCTTTGTTGGGTTTATACCACTTAGC	Sac II
1AB-A	1925~1949	GACGCGTCGACAGGTATCTGGTATGCTTCCATAGAG	Sac I
1C-S	1603~1627	GTCCCCGCGGACAACGTCACCCTAATGGTTATCCC	Sac II
1C-A	2843~2867	GACGCGTCGACGTGTGTTAGGATCTGTGCGTCTTGG	Sac I
1D-S	2359~2383	TCCCCGCGGGTTACATCATGTGTTTCGTGTCAGC	Sac II
1D-A	3391~3415	GACGCGTCGACAAGAGGTCTCTGTTGTAACTTTCCC	Sac I
2AB-S	3221~3245	TCCCCGCGGGGCAAAGAACGTGAACTTCCAACCC	Sac II
2AB-A	4073~4097	GACGCGTCGACTTCCATACCCTTGCAAGCATTCGTC	Sac I
2C-S	3777~3801	TCCCCGCGGGCATTCGGCTCCGGCTTTACTAACC	Sac II
2C-A	5094~5118	GACGCGTCGACTGTCTACCGATTTGAGCAGGTCCGC	Sac I
3ABC-S	4705~4729	TCCCCGCGGCCAATGCAGGATCTATTAATGCTCC	Sac II
3ABC-A	6015~6039	GACGCGTCGACTGAGTACTGCTGGTTCTTTGTTCCC	Sac I
3DUTR-S	5742~5766	GTCCCCGCGGGGTGGCACACCCACCAAGAGAATGC	Sac II
3DUTR-A	7372~7396	GACGCGTCGACCGCACCGAATGCGGAGAATTTACCC	Sac I

[a]"S" designates sense primer, and "A" designates anti-sense primer. [b]Additional bases were written in italics, and the restriction sites in primer were underlined.

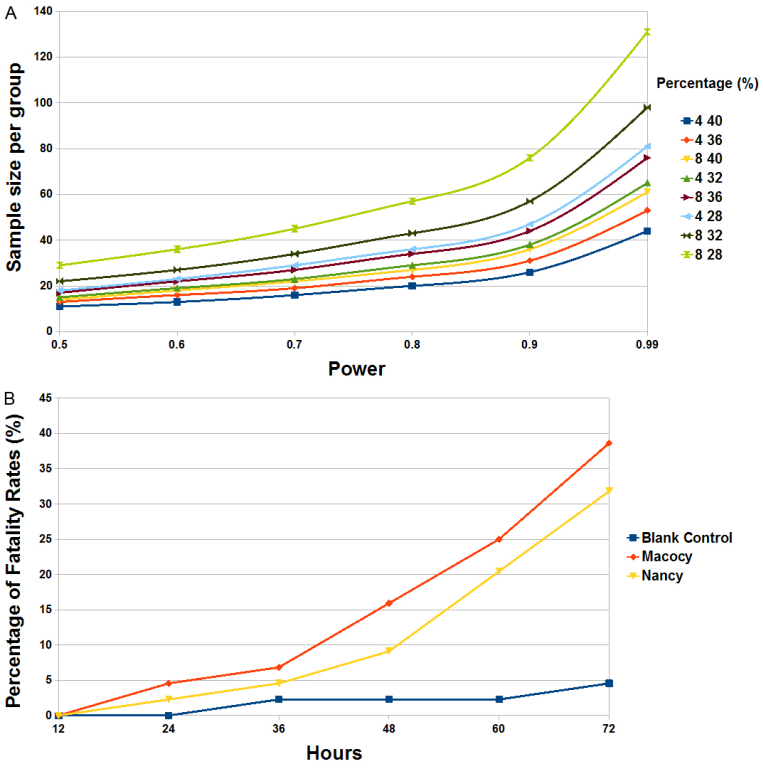

Figure 3. The sample size evaluation, fatality rates during 72 hours. A: 4% and 8% represent that of the control group, and 28-40% represents that of the CVB-inoculated groups. The death percentages' combinations of the control group and the CVB-inoculated groups were exhibited by different lines with different colors for evaluating the sample size per group with the power setting at 0.5-0.99. The sample size of 44 is chosen for the mouse model. B: CVB-inoculated mice were observed for fatality over a 72-hour period. Different line colors represent different groups.

sequence identity and lowest p distance with strain 28 rather than strain Nancy (**Table 2**), which means the new isolated Macocy strain is more like strain 28 rather than its parental strain Nancy from genomic view.

The sample size calculation with fatality in the study design

According to our previous study in our lab, the mice fatality rate of the CVB3-inoculated groups ranged from about 28% to 40%, while the natural fatality rate of the control group ranged from about 4% to 8%. With these fatality rates and the *power* of 0.99, the sample size of 44 to 131 per group was worked out. According to the estimation and many practical constraints, we chose 44 as an available sample size per group (**Figure 3A**). Further, the fatality rates of mice at 12-72 hours after inoculation were recorded every 12 hours. As

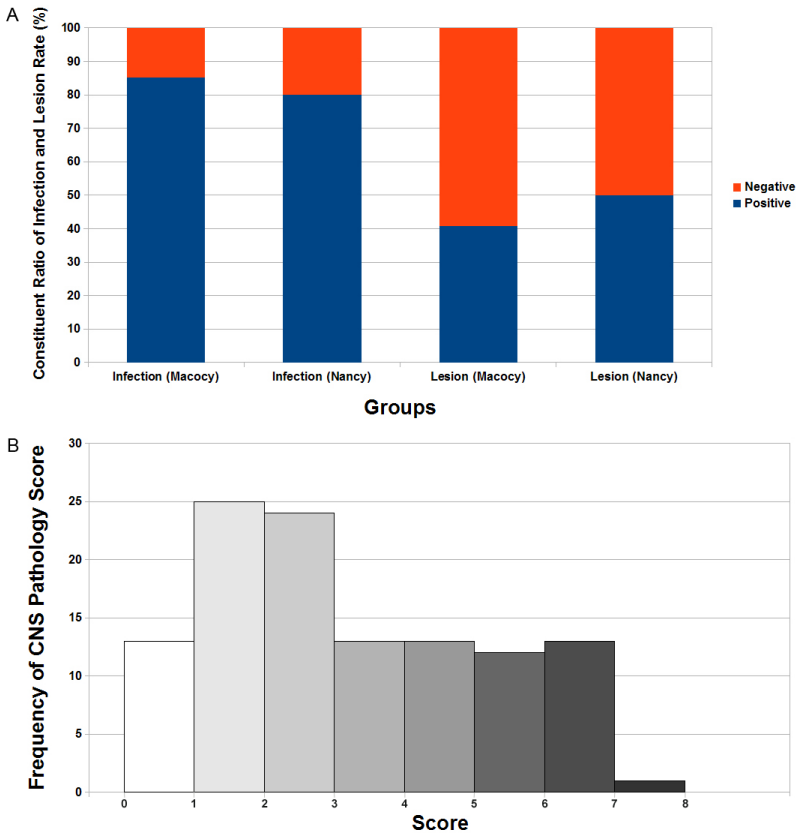

Figure 4. The infection and pathology rates constitution ratios as well as the frequency distribution of score. A: The infection rates as well as negative percentages of IHC on both group Macocy and Nancy were exhibited on the stacked column, while the positive lesion rates as well as negative rates on both groups were exhibited on the stacked column. B: The bar chart shows the frequency distribution of pathology score for CNS pathology. The score ranges 0 to 8, and the y-axis shows the frequency of every score.

time passed by, the fatality rates at the 72nd hour in the control group, group Nancy and group Macocy were rising to 4.55% (2 deaths), 31.82% (14 deaths) and 38.64% (17 deaths) respectively (**Figure 3B**). The fatality rates of infected groups are very highly significant [23] for both group Nancy ($p<0.001$) and group Macocy ($p<0.001$). Hence, this suggested that it is the virus infection (5×10^5 $TCID_{50}$/ml) induces the fatality of neonatal mice. Furthermore, the minimum sample size of 22 per group for hematoxylin & eosin (H&E) staining and immunohistochemistry (IHC) assay was calculated with the *power* setting at 0.99, the positive proportion setting at 0.05 in the control group, and the positive proportion setting at 0.60 in each of the virus-inoculated group. Consequently, the survival mice in group Nancy (30), group Macocy (27) and the control (22) were dissected for pathological assay.

The infection rate and pathology rate of strain Macocy and Nancy

IHC assay demonstrated CVB3 had infected the brain tissue of neonatal mice with the positive rate of 85.19% in group Macocy, 80.00% in group Nancy and the pathological lesion rate of 40.74% in group Macocy, 50.00% in group Nancy (**Figure 4A**). On all of the brain tissue samples, the median of pathology score is 2 and the mode is 1. The score range is from 0 to 7, and there are >10% samples were scored 6-7 (**Figure 4B**). The association between CVB3 infection and the virus inoculation are very highly significant for both group Nancy ($p<0.001$) and group Macocy ($p<0.001$).

There is no difference between strain Macocy and Nancy

Comparing the fatality rates of mice at the 72nd hour for group Macocy versus group Nancy, we found there is no significant difference ($p<0.503$, *power*<0.102, **Figure 7C**). Further, we found there is no difference between strain Macocy and Nancy in CNS infection ($p<0.734$, *power*<0.053) and pathological lesion ($p<0.483$, *power*<0.107, **Figure 7D**), Comparing the infection rate in group Macocy and Nancy. The result confirmed by the low power which shows there is virtually no chance to find a significant difference. Therefore, the mutation between strain Macocy and its parental strain Nancy does not change the pathology of CNS infection.

CVB-induced CNS pathology

DAB staining distribution demonstrated that the CVB widely spread on brain tissue, in which we carefully checked cerebral cortex and hippocampus region respectively. CVB have infect-

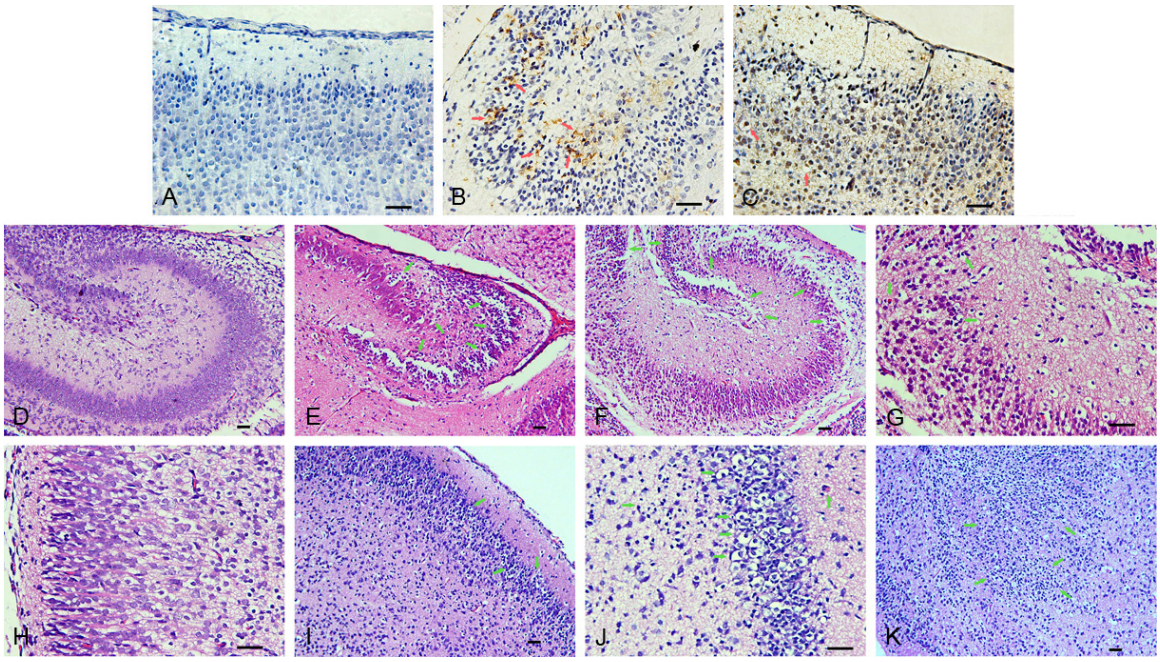

Figure 5. Pathological changes of brain in CVB infected mice at the disease onset phase. Images (A-C) display the IHC stained slices of brain, in which image (A) is a control picture from the brain cortex region. Brown (B and C) represents CVB. The arrows (B and C) point some of the dead cells with IHC positive staining. Image (B) comes from the brain hippocampal dentate gyrus region, while image (C) from the brain cortex. Images (D-G) display the H&E stained slices of brain hippocampal dentate gyrus regions, in which image (D) shows the normal state, while images (E-G) show the pathology lesion of this region. The arrows (E-G) point some of the dead cells and inflammatory cells. Image (G) is a magnified photograph of image (F). Images (H-K) display the H&E stained slices of brain cortex, in which image (H) shows the normal state, while images (I-K) show the pathology nidus. The arrows point some of the dead cells (I) and the accumulation area of massive inflammatory cells (J and K). All the bars in the histological pictures represent 50 μm.

ed the hippocampus regions and cortex regions (**Figure 5B**, **5C**) and induced pathological lesion in these areas (**Figure 5E-G**, **5I-K**). Neurons were extensively damaged in hippocampus region, and in some samples, the dentate gyrus region was almost destroyed by CVB3 completely (**Figure 5E**). Many of the dead cells had a condensed nucleus. At the same time, large amount of inflammatory cell infiltrated the damaged tissue (**Figure 5E-G**). In the cerebral cortex, from molecular layer, external granular layer to polymorphous cell layer, extensively cellular damage could also be found. The same as the hippocampus region, condensed nucleus and inflammatory cell could also be clearly observed in cerebral cortex (**Figure 5I-K**). Feuer R et al. has reported that CVB3 infection can induce neuron apoptosis in hippocampus [8]. In our H&E staining slices, neuron apoptosis also can be identified with the signs of cytoplasm eosinophilic staining, karyopyknosis, nucleus marginalization and the separation of cell body from the nearby cells. Microglias infiltrated the small nidus and surrounded the degenerative neurons (**Figure 5J**). But, judging from all the samples, the phenomena above is not very common. In fact, most cases here showed that the damaged neurons in the nidus were not crowded with so many microglias. It can be sure some of mice suffered encephalitis.

The track of CVB penetrating BBB

We also have shot some interesting photographs that CVB in blood vessel were trying to penetrate the BBB at the cortex and the track is shown in **Figure 6**. In these pictures, the CVB staining was crowded in the blood vessel. It were detected on the two side of BBB, and a little of CVB were also detected by staining in the layer nearby the BBB. The CVB staining defused along the nerve fiber and radiated from the vessel. This is a firm evidence that CVB, as a member of enterovirus, can break through the BBB to infect the CNS in vivo. On the other side, the track of coxsackievirus

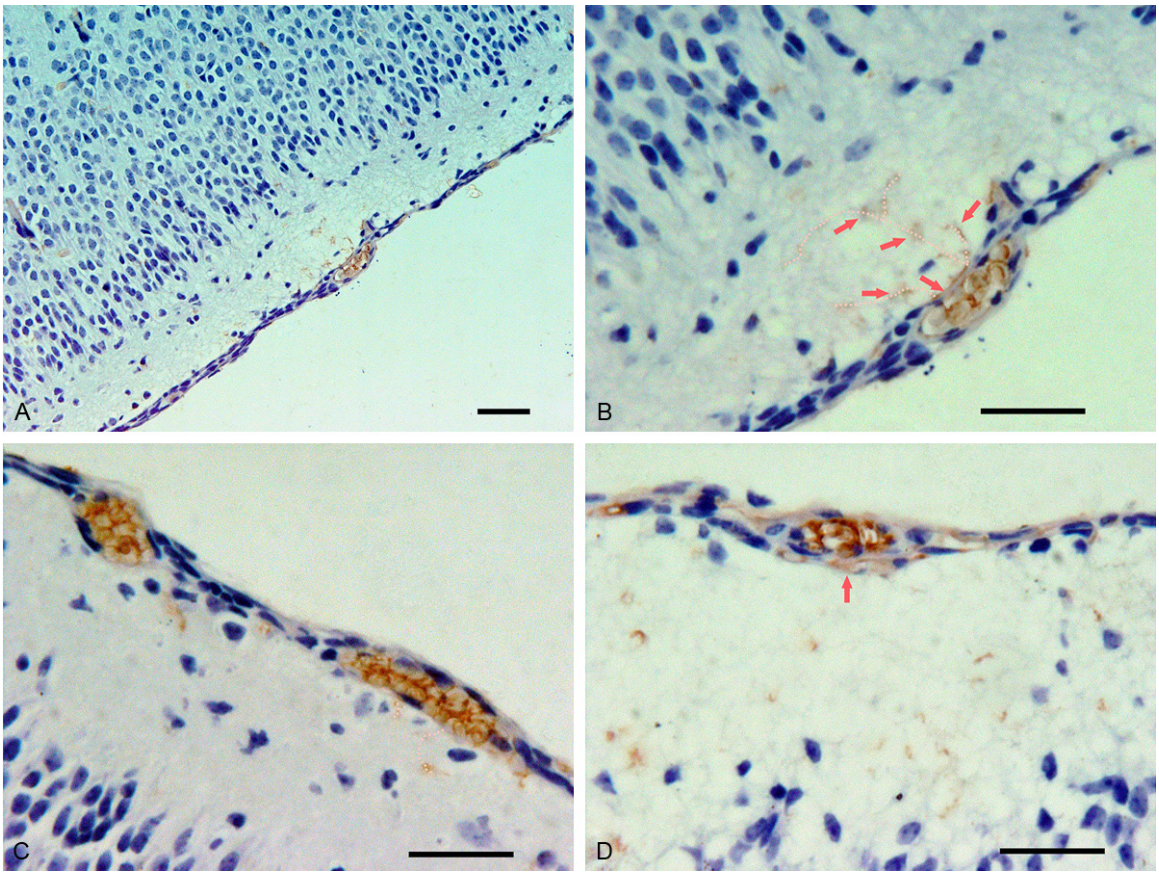

Figure 6. The process of CVB penetrating the BBB. Images (A-D) display the IHC stained slices of brain cortex. Brown (A and B) shows the CVB staining. Image (B) is a magnified photograph of image (A) at one blood capillary. The arrows (B) point the BBB and the positive staining of CVB. The dash lines describe the general penetrating track of CVB. Another two blood capillaries (C and D) have been shown, with dash lines describing the general penetrating track of CVB. Image (D) has been shown a blood capillary without CVB breaking through the BBB. The arrow points the BBB and the blood capillary. All the bars in the pictures represent 50 μm.

infecting brain tissue can be somewhat blocked by BBB.

Discussion

Coxsackievirus B could cause serious CNS infection. In this study, we used a classical clinical CVB3 strain Nancy and a newly isolated CVB3 strain Macocy to develop the CNS disease mouse model. To imitate the infecting situation of the newborn infection by CVB in the first 1-2 weeks, we chose the newborn mice within 24 hours, and randomly separated them into two groups. These neonatal mice were infected by feeding, which is a natural way for CVB epidemically spread and infect [24].

The *power* of the statistical tests was calculated, which tells us how many chances of rejecting null hypothesis when alternative hypothesis is true. Generally, the *power* of greater than 0.7 reveals the probability of finding the significance is large, while the *power* of less than 0.6 reveals the probability is small. The high *power* indicates it is highly likely to be sure of the fatality and infection of virus-inoculated groups, which ensures the solidity of the mouse model (**Figure 7**).

Feuer et al. have tried to establish the CVB3 infection model of encephalitis by feeding at 2003. But they failed, and established the model by intracranial injection instead [8]. We noted that they returned the mice to their mothers after the mice were inoculated virus. Because the enterovirus infection risk is associated with the lack of breast feeding [25], we do it differently in this step. After inoculation, we fed the mice with sterile milk manually and took care of the mice by ourselves rather than return them to their mothers. At last, it is obvi-

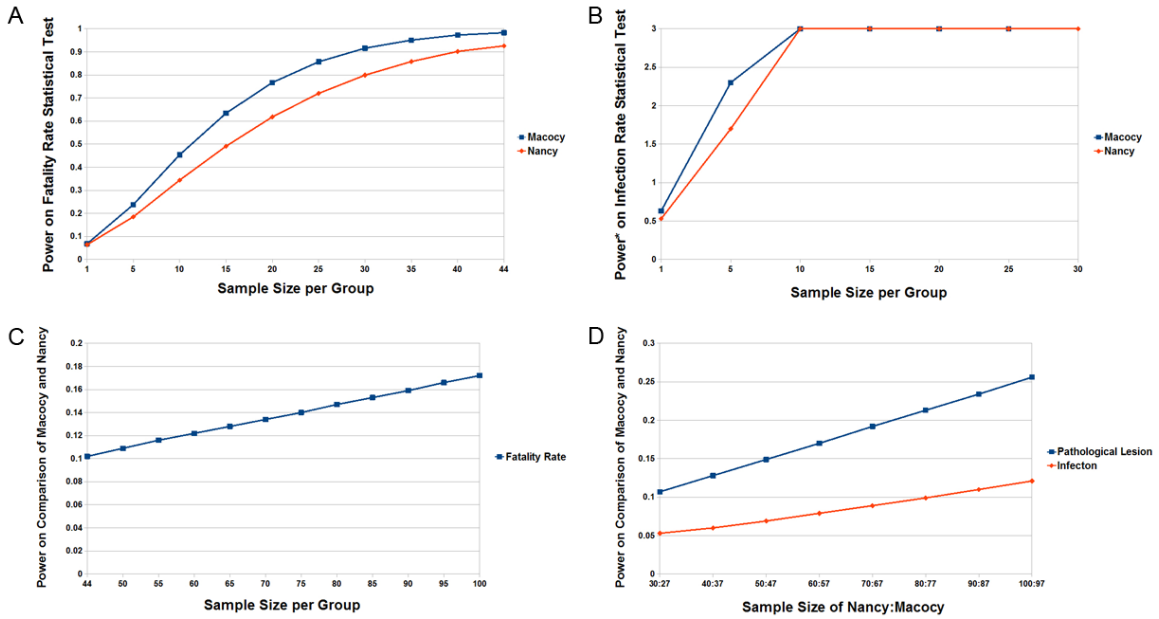

Figure 7. The trends of powers on statistical tests. A: The two lines show the trend of power for the fatality rates of group Macocy and Nancy, as the sample size is arising. B: The two color lines show the trend of power for the infection of group Macocy and Nancy, as the sample size is arising. The power* represents the mathematically changed power by $\log_{10}\frac{1}{1-x}$, in which x = *power* and power * = $\log_{10}\frac{1}{1-x}$. To illustrate, power* of 0.53 equals power of 0.71, power* of 3 equals power of 0.99 and so on. C: The line shows the trend of power for comparing the fatality rates of group Macocy and Nancy, as the sample size is arising. D: The two color lines show the trend of power for comparing the infection and lesion of group Macocy and Nancy, as the sample size is arising.

ous that the acute encephalitis model on neonatal mice was successfully established.

As a matter of fact, the brain is protected by the BBB and this barrier is made up of three layers, which are named endothelial cell layers, capillary basement membrane and astrocyte endfeet. It is believed that all the three layers are necessary for the function of BBB [26]. Recently, Coyne et al have proposed that CVB can access the CNS through the BBB endothelium to cause aseptic meningitis based on in vitro model of BBB endothelium [16]. However, the BBB is composed of three layers not only the endothelium. In our research, we captured the process of CVB penetrating the BBB in vivo (**Figure 6**). This result shows the track of CVB accessing the brain. Our result also showed that the infection process can be somewhat blocked by BBB (**Figure 6D**). So the BBB protection is still effective although it cannot stop CVB infection completely.

There are extensive reports that hippocampal pathology is related to clinically neuropsychiatric illnesses, including amnesia, dementia, and epilepsy [9, 27, 28]. In the meantime, recent studies on schizophrenia have found the evidence for abnormalities of hippocampal structure and function, especially dentate gyrus [10, 29-31]. For another, cortex pathology induced by CVB may contribute to seizures following acute viral infection [11, 32]. CVB5 has been reported that could clearly increase the risk of onset of schizophrenia on adult if infection happened during the newborn period [1]. In addition, there were epidemiological surveys revealed congenital enterovirus infection has been epidemiologically implicated as a possible cause of schizophrenia [12, 13]. Hence, the hippocampal pathology, especially dentate gyrus damage, and cortex regions by CVB may be one possible way for enterovirus-induced schizophrenia and other neuropsychiatric illness. Our histological evidence and the orally infected mouse model could well promote the related researches.

Acknowledgements

This study was supported by the grant (2009-ZX09301-014-1) awarded by National Mega

Project on Major Drug Development (People's Republic of China).

Disclosure of conflict of interest

All the authors declare that they have no competing interests.

Address correspondence to: Changyuan Dong or Zhen Song, Laboratory of Molecular Virus & Cancer, State Key Laboratory of Virology, Wuhan University School of Basic Medicine, Wuhan 430071, China. E-mail: dongchangyuan2008@163.com (Changyuan Dong); tonysong.whu@gmail.com (Zhen Song)

References

[1] Stanway G, Brown F, Christian P, Hovi T, Hyypiä T, King AMQ, Knowles NJ, Lemon SM, Minor PD, Pallansch MA, Palmenberg AC, Skern T. Family Picornaviridae. In: Fauquet CM, Mayo MA, Maniloff J, Desselberger U, Ball LA (ed). Virus Taxonomy Eighth Report of the International Committee on Taxonomy of Viruses. London: Elsevier Academic Press, 2005; pp: 757-778.

[2] Berlin LE, Rorabaugh ML, Heldrich F, Roberts K, Doran T, Modlin JF. Aseptic meningitis in infants <2 years of age: diagnosis and etiology. J Infect Dis 1993; 168: 888-892.

[3] Khetsuriani N, Lamonte-Fowlkes A, Oberst S, Pallansch MA. Centers for Disease Control and Prevention: Enterovirus surveillance--United States, 1970-2005. MMWR Surveill Summ 2006; 55: 1-20.

[4] Khetsuriani N, Quiroz ES, Holman RC, Anderson LJ. Viral meningitis-associated hospitalizations in the United States, 1988-1999. Neuroepidemiology 2003; 22: 345-52.

[5] Romero JR. Pediatric Group B Coxsackievirus Infections. In: Tracy S, Oberste MS, Drescher KM (ed). Group B Coxsackieviruses. Heidelberg: Springer-Verlag, 2008; pp: 223-240.

[6] Fairweather D, Rose NR. Coxsackievirus-induced myocarditis in mice: a model of autoimmune disease for studying immunotoxicity. Methods 2007; 41: 118-22.

[7] Vargová A, Bopegamage S, Borsanyiová M, Petrovicová A, Benkovicová M. Coxsackievirus infection of mice. II. Viral kinetics and histopathological changes in mice experimentally infected with coxsackievirus B3 by intraperitoneal route. Acta Virol 2003; 47: 253-257.

[8] Feuer R, Mena I, Pagarigan RR, Harkins S, Hassett DE, Whitton JL. Coxsackievirus B3 and the neonatal CNS: the roles of stem cells, developing neurons, and apoptosis in infection, viral dissemination, and disease. Am J Pathol 2003; 163: 1379-1393.

[9] Cipolotti L and Bird CM. Amnesia and the hippocampus. Curr Opin Neurol 2006; 19: 593-598.

[10] Heckers S and Konradi C. Hippocampal pathology in schizophrenia. Curr Top Behav Neurosci 2010; 4: 529-553.

[11] Härtel C, Schilling S, Gottschalk S, Sperner J. Isolated unilateral cortical oedema and complex partial seizures in association with coxsackievirus B infection. Epilepsy Behav 2002; 3: 480-482.

[12] Rantakallio P, Jones P, Moring J, Von Wendt L. Association between central nervous system infections during childhood and adult onset schizophrenia and other psychoses: a 28-year follow-up. Int J Epidemiol 1997; 26: 837-843.

[13] Eagles JM. Are polioviruses a cause of schizophrenia. Br J Psychiatry 1992; 160: 598-600.

[14] Coyne CB and Bergelson JM. Virus-induced Abl and Fyn kinase signals permit coxsackievirus entry through epithelial tight junctions. Cell 2006; 124: 119-131.

[15] Coyne CB, Kim KS, Bergelson JM. Poliovirus entry into human brain microvascular cells requires receptor-induced activation of SHP-2. EMBO J 2007; 26: 4016-4028.

[16] Coyne CB, Bozym R, Morosky SA, Hanna SL, Mukherjee A, Tudor M, Kim KS, Cherry S. Comparative RNAi screening reveals host factors involved in enterovirus infection of polarized endothelial monolayers. Cell Host Microbe 2011; 9: 70-82.

[17] Hall TA. BioEdit: a user-friendly biological sequence alignment editor and analysis program for Windows 95/98/NT. Nucl Acids Symp Ser 1999; 41: 95-98.

[18] Tamura K, Peterson D, Peterson N, Stecher G, Nei M and Kumar S. MEGA5: Molecular Evolutionary Genetics Analysis using Maximum Likelihood, Evolutionary Distance, and Maximum Parsimony Methods. Mol Biol Evol 2011; 28: 2731-2739.

[19] Diegert C, Diegert KV. Note on Inversion of Casagrande-Pike-Smith Approximate Sample-Size Formula for Fisher-Irwin Test on 2×2 Tables. Biometrics 1981; 37: 595.

[20] Fleiss JL, Tytun A, Ury HK. A Simple Approximation for Calculating Sample Sizes for Comparing Independent Proportions. Biometrics 1980; 36: 343-346.

[21] Walters DE. In defense of the arc sine approximation. Journal of the Royal Statistical Society 1979; 28: 219-222.

[22] Yang Z. Computational molecular evolution. New York: Oxford University Press, 2006; pp: 3.

[23] Rosner B. Fundamentals of Biostatistics. 5th ed. Duxbury, CA, 2000; pp: 555.

[24] Tracy S and Gauntt C. Group B Coxsackievirus Virulence. Curr Top Microbiol Immunol 2008; 323: 149-163.

[25] Jenista JA, Powell KR, Menegus MA. Epidemiology of neonatal enterovirus infection. J Pediatr 1984; 104: 685-690.
[26] Ballabh P, Braun A, Nedergaard M. The blood-brain barrier: an overview: structure, regulation, and clinical implications. Neurobiol Dis 2004; 16: 1-13.
[27] Korf J, Gramsbergen JB. Hippocampus pathology in dementia: post-mortem assessed cation shifts and amino acid transmitter contents and its possible neuroimaging in vivo. Electroencephalogr Clin Neurophysiol Suppl 1991; 42: 366-79.
[28] Weber B, Wellmer J, Reuber M, Mormann F, Weis S, Urbach H, Ruhlmann J, Elger CE, Fernández G. Left hippocampal pathology is associated with atypical language lateralization in patients with focal epilepsy. Brain 2006; 129: 346-351.
[29] Knable MB, Barci BM, Webster MJ, Meador-Woodruff J, Torrey EF. Molecular abnormalities of the hippocampus in severe psychiatric illness: postmortem findings from the Stanley Neuropathology Consortium. Mol Psychiatry 2004; 9: 609-620.
[30] Lauer M, Beckmann H, Senitz D. Increased frequency of dentate granule cells with basal dendrites in the hippocampal formation of schizophrenics. Psychiatry Res 2003; 122: 89-97.
[31] Reif A, Fritzen S, Finger M, Strobel A, Lauer M, Schmitt A, Lesch KP. Neural stem cell proliferation is decreased in schizophrenia, but not in depression. Mol Psychiatry 2006; 11: 514-522.
[32] Fujita Y, Imai Y, Ishii W, Endo A, Arakawa C, Kohira R, Fuchigami T, Okubo O, Mugishima H. Improvement of intractable childhood epilepsy following acute viral infection. Brain Dev 2011; 33: 62-68.